

MODELLING DEM DATA UNCERTAINTIES FOR MONTE CARLO SIMULATIONS OF ICE SHEET MODELS

Felix Hebeler and Ross S. Purves

Department of Geography
University of Zurich
8057 Zurich, Switzerland
fheberer@geo.unizh.ch, rsp@geo.unizh.ch

KEY WORDS: GIS, DEM/DTM, Error, Correlation, Impact Analysis, Modelling, Reference Data, Glaciology

ABSTRACT:

For realistic modelling of digital elevation model (DEM) uncertainty, information on the amount and spatial configuration is needed. However, common DEM products are often distributed with global error figures at best. Where no higher accuracy reference data is available, assumptions have to be made about the spatial distribution of uncertainty, that are often unrealistic. In order to assess the impact of DEM uncertainty on the results of an ice sheet model (ISM) for an area where no higher accuracy reference data was available, we quantified DEM error of comparable regions with available reference data. Deriving good correlation of error magnitude and spatial configuration with DEM characteristics, these dependencies were incorporated into an uncertainty model containing both deterministic and stochastic components. The developed uncertainty model proved to reproduce amount and spatial correlation of DEM error well while producing uncertainty surfaces suitable for Monte Carlo Simulations (MCS). Applying the model to a DEM of Fennoscandia, a MCS was conducted using an ISM during the first 40ka of the Last Glacial Maximum (LGM). Results showed DEM uncertainty to have significant impact on model results during nucleation and retreat of the ice sheet.

1 INTRODUCTION

All modelling is susceptible to the introduction of uncertainties to model results throughout the modelling chain. During data acquisition systematic error, measurement imprecision or limited accuracy of sensors can introduce ambiguities to measured values. Preprocessing and preparation of data to meet model needs, such as reprojecting, scaling or resampling the data introduces uncertainty. Finally, the methods and algorithms used as well as effects such as computational precision during modelling can introduce further uncertainties to results.

As all modelling is a mere abstraction of much more complex processes, that in many cases might not be fully understood, uncertainties are also an intrinsic part of the approach. Uncertainties are thus not necessarily a problem in modelling, but rather an inherent component of the process, as long as the sources and bounds of the uncertainties associated with individual models are known and understood. Where this is the case, sensitivity tests can be conducted to assess the susceptibility of model results to uncertainties in certain data, parameters or algorithms and compare these uncertainties with the sensitivity of model runs to variations in individual parameters. Decision makers have become increasingly familiar with such methodologies, through for example the scenarios presented in IPCC reports (IPCC, 2001).

While uncertainties inherent in spatial data have been the focus of a number of research projects in the GIScience community, many users of spatial data either completely neglect this source of uncertainty or consider it less important than for example, parameter uncertainties. However, even if a modeller is aware of the uncertainties introduced through, for instance a Digital Elevation Model (DEM), it is not always straightforward or even possible to assess them, e.g. when metadata from the data producers is incomplete, incorrect or missing. If this information cannot be reconstructed, assumptions have to be made that might or might not be realistic and sensible for testing the impact of uncertainties in spatial data on a model.

In this paper, we use the term 'error' when referring to the deviation of a measurement from its true value. This implies that

elevation error of a DEM can only be assessed where higher accuracy reference data is available (Fisher and Tate, 2006). Error is inherent in any DEM, but is usually not known in terms of both magnitude and spatial distribution, thus creating uncertainty. 'Uncertainty' is used in this context, where a value is expected to deviate from its true measure, but the extent to which it deviates is unknown, and can only be approximated using uncertainty models (Holmes et al., 2000).

1.1 Motivation

Ice sheet models, which are commonly used to explore the linkage between climate and ice extent either during past glacial periods, or to explore the response of the Earth's remaining large ice masses (the Greenland Ice Cap and the Antarctic Ice Sheet) to future climate change, run at relatively low resolutions of the order of 1-20km, for a number of reasons. Since the models run at continental or even global scales, computational capacities as well as assumptions in model physics limit possible modelling resolutions. Furthermore, climate models used to drive such models commonly run at even lower resolutions, and until recently the highest resolution global topographic datasets had nominal resolutions of the order of 1km. Ice sheet modellers commonly resample the highest available resolution data to model resolutions - for example in modelling ice extents in Patagonia a 1km resolution DEM was resampled to 10 and 20km respectively (Purves and Hulton, 2000). While it is often assumed that data accuracy of 1km source data is essentially irrelevant when resampled to 10 or 20km, previous work has suggested that these uncertainties can have a significant impact on modelled ice sheet extents and volumes (Hebeler and Purves, 2005).

Despite the recognised need (Kyriakidis et al., 1999), most DEM data is still distributed with little metadata - usually at best global values such as RMSE or standard deviation of error are given (Fisher and Tate, 2006). Information on spatial distribution of uncertainties is almost always not available, and assumptions made about the distribution of uncertainties are often debatable (Fisher and Tate, 2006, Wechsler, 2006, Oksanen and Sarjakoski, 2005, Weng, 2002, Holmes et al., 2000).

Following the approach of Hagdorn (2003) in reconstructing the Fennoscandian ice sheet during the last glacial maximum (LGM), we wanted to test the sensitivity of the model results to DEM data uncertainty. Hagdorn used GLOBE DEM data as input topography, for which accuracy figures are given as global values depending on the data source e.g. vertical accuracy of 30m at the 90% confidence interval for data derived from DTED (Hastings and Dunbar, 1998), with no information on spatial configuration or dependencies of uncertainties or error. Thus in order to assess the impact of uncertainty in the DEM on the ISM, a realistic model of GLOBE DEM uncertainty must also be developed which both describes dependencies of error values on the DEM and sensibly reconstructs the spatial configuration of uncertainty.

1.2 Aims

In this paper we set out to address three broad aims, which can be described as follows:

- To quantify the error in DEMs for a range of appropriate regions, using higher resolution data, and to assess the extent to which this error correlates with DEM characteristics.
- To develop a general model of DEM error for use in areas where higher resolution data are not available and simulate the spatial and numerical distribution of the remaining uncertainty stochastically.
- To apply the DEM uncertainty model in Monte Carlo Simulations of ISM runs for Hagdorn’s experiments (Hagdorn, 2003) and assess the impact of modelled topographic uncertainty on ISM results.

The third aim can thus be considered as a case study of the application of a set of general techniques aimed at modelling DEM uncertainties and allowing their impact on model results to be compared with other potential sources of uncertainty.

2 MATERIALS & METHODS

The availability of SRTM data makes the evaluation of GLOBE and GTOPO30 data accuracy possible for large areas of the globe (Jarvis et al., 2004, Harding et al., 1999), and thus it is possible to retrospectively evaluate previous experiments that used GLOBE DEM as input data. However, since our study area of Fennoscandia lies outside the region covered by SRTM data (CIAT, 2006), no direct assessment of error using higher accuracy reference data is possible.

Our approach was thus as follows. Firstly, regions with similar topography and data sources to Fennoscandia, but lying within regions covered by SRTM data were identified. Secondly, error surfaces were generated by assuming the SRTM data to be a higher quality data source for these regions. A model of error, incorporating a stochastic component, which represents a generalised uncertainty model for all regions was then developed. Using this model it is possible to perform MCS simulations with the ISM, since the stochastic component of the uncertainty model means that multiple uncertainty surfaces can be generated.

2.1 DEM data

For the analysis of typical GLOBE DEM uncertainty, three datasets were selected based on previous tests which showed that uncertainty in the GLOBE DEM data was highest in high altitude and high relief areas. Such areas are also central to ice sheet inception (Marshall, 2002, Sugden et al., 2002) and thus likely to be particularly susceptible to uncertainty. To derive the uncertainty

DEM	Alps	Pyrenees	Turkey	Scand
Altitude	1 - 4570m	1 - 3276m	1 - 4938m	0 - 2191m
Mean	692.8m	651.9m	1066.5m	189.5m
STD	624.8m	481.2m	738.4m	207.4m
Skewness	1.65	0.86	0.55	3.09
Kurtosis	5.46	3.86	2.29	15.0
Source	DTED*	DTED	DTED	DTED
Size (cells)	1083108	720000	816837	6094816

Table 1: Descriptive statistics for the three test areas and the Fennoscandian study site used. * *Italian data provided by Servizio Geologico Nazionale (SGN) of Italy.*

model for Fennoscandia, GLOBE data for the European Alps, the Pyrenees and the eastern part of Turkey were selected. These regions have relatively similar properties in terms of hypsometry (Fig. 1) and statistics describing elevation values (Table 1) and were all compiled from DTED data, with the exception of the Italian part of Alps where data were sourced from the Italian national mapping agency (Hastings and Dunbar, 1998). For

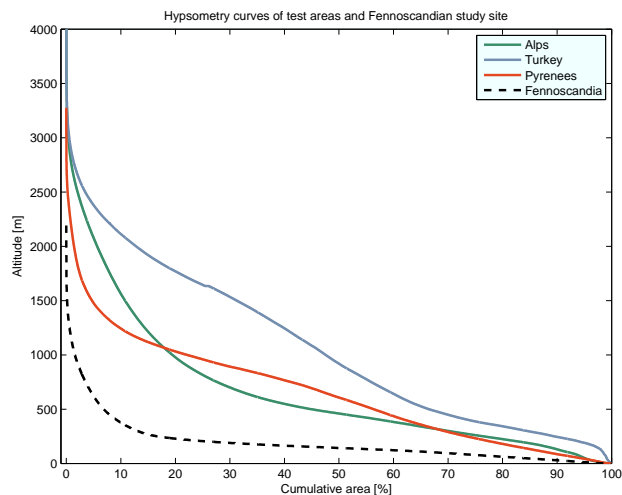


Figure 1: Hypsometry of the three selected test areas (solid lines) and the Fennoscandian study area (dashed), calculated from GLOBE DEM data at 1km resolution. Test areas show relative large proportions of the high areas that are of interest in the study site DEM of Fennoscandia. Altitudes above 4000m cropped for better visibility.

the three selected test areas, hole-filled SRTM data at 100m resolution (CIAT, 2006) were resampled to align with the GLOBE DEM at 1km resolution (GLOBE Task Team & others, 1999), using the mean of all SRTM cells within the bounds of the corresponding GLOBE data cell (Jarvis et al., 2004). Waterbodies were eliminated from all datasets, and error surfaces for the respective test areas were calculated by subtracting the GLOBE data from the averaged SRTM data. SRTM data in this approach is thus used as ground truth and considered error free. Like any data source, SRTM does of course contain errors (Sun et al., 2003, Heipke et al., 2002) - however their magnitude and spatial distribution was considered negligible for this experiment. Calculations on the data sets were conducted using the original, unprojected WGS84 spatial reference which both SRTM and GLOBE DEM data are distributed in. For calculation of slope and related parameters, all DEMs were projected to Albers Equal Area projections (using WGS84 geoid), with the projection parameters chosen to minimise distortion for every region and minimise any further uncertainty introduced by the process (Montgomery, 2001).

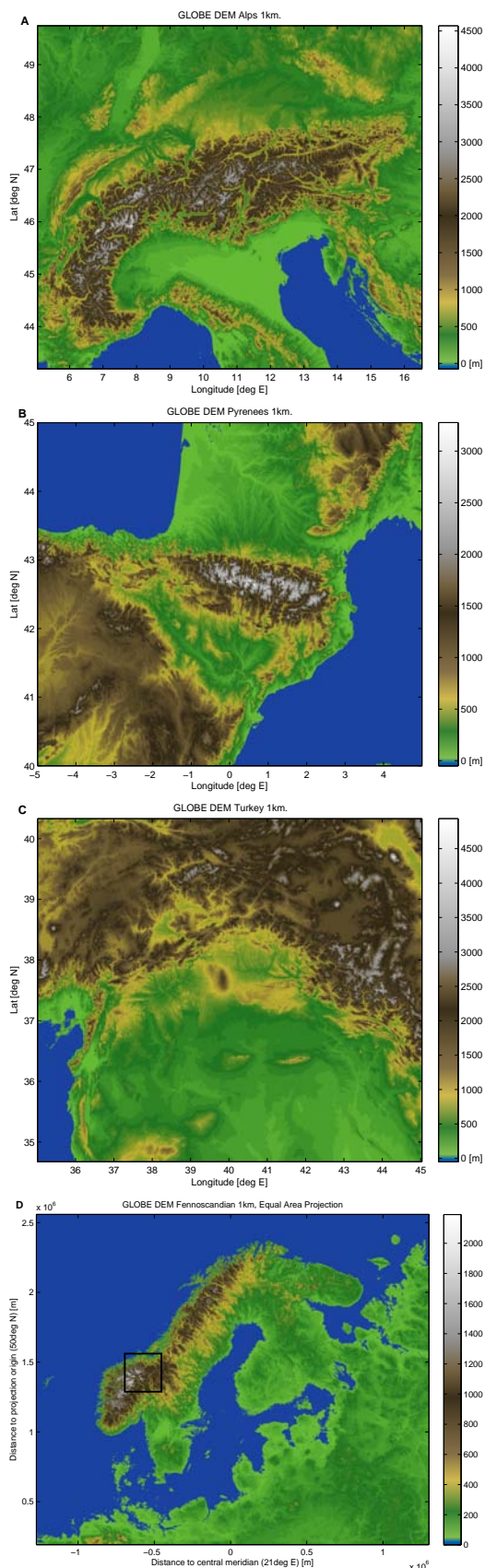


Figure 2: GLOBE DEM of the three test areas and the study site at 1km resolution. From top to bottom: (A) Alps, (B) Pyrenees, (C) Turkey (WGS84), (D) Fennoscandia (AEA).

2.2 Uncertainty model

Having derived error surfaces, they were first visually inspected. Descriptive statistics were calculated for each of the three areas and hypsometric curves and histograms compared. To assess spatial autocorrelation of both the DEM and the calculated error surfaces, semivariogram maps were derived for both the complete data sets as well as characteristic regions (e.g. for areas with high relief). Additionally, local Moran's I was calculated for all surfaces (Wood, 1996). Error, error magnitude and error sign were then tested for correlation with a set of terrain attributes and parameters (Table 2), where all neighbourhood analysis was conducted with a 3x3 window, which was found in to give the highest correlation values in pre-tests. Stepwise regression anal-

Altitude	Value of GLOBE cell
Error	Deviation of GLOBE from mean SRTM value
Error Magnitude	Magnitude of error
Sign	Sign of error (+1/-1)
Aspect	Direction of first derivative of elevation
Slope	Magnitude of first derivative of elevation
Plan Curvature	2nd derivative orthogonal to direction of steepest slope
Profile Curvature	2nd derivative in direction of steepest slope
Total Curvature	Compound curvature index
Maximum-Mean- extremity Minimum-	Deviation of center cell from max/mean/min of 3x3 neighbourhood
Roughness (Altitude)	Standard deviation of altitude in a 3x3 neighbourhood
Roughness (Slope)	Standard deviation of slope in a 3x3 neighbourhood

Table 2: Attributes, derivatives and indices used during correlation analysis. Extremity index calculated after Carlisle (2000).

ysis was used to find the best descriptive variables for modelling error in each of the three testing areas. The derived regression factors were averaged to formulate a general regression model for all three areas. Using this general regression, the residuals for each of the areas were also analysed to assess their dependency on the properties of the original DEM (Table 2). Again, a method to reproduce the characteristics common to the residuals of all three test area was sought, and combined with the first regression equation. In order to reproduce the spatial autocorrelation encountered in the original error surfaces, the uncertainty surfaces modelled using the above method were then transformed to a normal distribution and filtered using a Gaussian convolution filter (Ehlschlaeger et al., 1997, Hunter and Goodchild, 1997) using kernel sizes derived from autocorrelation analysis of the original error surfaces. The modelled uncertainty surfaces were next compared with the derived true error surfaces in terms of both their spatial and statistical distribution.

The developed uncertainty model was used to calculate a suite of 100 uncertainty surfaces for Fennoscandia that were superimposed on the original GLOBE DEM and used as input topographies for a MCS using the ISM.

2.3 Ice Sheet Model runs

The ISM used in these experiments is the GLIMMER model (Hagdorn et al., 2006), which was developed as part of GENIE (Grid Enabled Integrated Earth system model) and is freely available. For our experiments, we followed the approach of (Hagdorn, 2003) and ran simulations at 10km resolution for the 40 thousand years from approximately 120ka to 80ka BP. Climate forcing (essentially describing temperature and input mass) is based on an equilibrium line altitude (ELA) parameterisation (The ELA is the altitude at which net accumulation is zero - above the

	Range	Mean	STD	Skew.	Kurt.
Alps	-1140-1169m	3.3m	82.2m	0.05	11.61
Pyrenees	-920-797m	4.2m	68.8m	-0.14	14.23
Turkey	-817-964m	3.0m	70.7m	-0.04	11.29

Table 3: Descriptive statistics of derived GLOBE DEM error from three test areas.

Error Magnitude	Alps	Pyrenees	Turkey
Local Model	0.441	0.406	0.423
Global Model	0.430	0.393	0.422

Table 4: r^2 values of the regression modelling the amount of error for the three test areas. The good fit using the regression coefficients of the local model (top row) is retained when using the averaged global coefficients on each of the three areas (bottom row).

ELA mass accumulates, and below it ablates) derived from the Greenland ice core project (GRIP) data. Model runs have a time step of one year, and simulated ice thickness (and thus extents) are output to file every 500 years. Input topographies for the GLIMMER simulations consist of the GLOBE DEM data with added uncertainty surfaces derived from 1km uncertainty surfaces created by the uncertainty model, projected to Albers Equal Area projection and resampled to 10km resolution using bilinear interpolation. This method was chosen as it is a standard resampling technique applied by ice sheet modellers, and therefore is more representative for the study than the method of averaging of all contribution cells used in resampling SRTM to 1km (compare section 2.1).

3 RESULTS

3.1 Uncertainty model

Error properties Initial visual inspection of the derived error surfaces shows the high spatial correlation of error along prominent terrain features within the data set (compare Figures 2a and 3a), with reduced autocorrelation in areas of low relief. The distribution of error magnitude and sign also suggests some error dependencies on data sources, most visible through the lower overall error in the Italian part of the Alps seen in Figure 3a. Global autocorrelation analysis using semivariogram maps showed the range of autocorrelation to lie between 2 and 4km for each dataset, with directional trends following the orientation of prominent terrain features in the original DEMs. These semivariogram maps are strongly influenced by the semivariogram properties of high relief areas, since areas of low relief show little to no spatial autocorrelation at these resolutions. Calculated values of local Moran's I reinforce these findings. The statistic distribution of error (Table 3) shows comparable distributions for all three areas.

Error correlation Correlation analysis of error with the parameters presented in Table 2 showed relatively weak correlations with coefficients of between 0.2 and 0.5 for mean extremity, curvature and aspect for all datasets. Testing the magnitude of error for correlation resulted in higher correlation coefficients for minimum extremity, roughness of altitude, slope and altitude with values of up to 0.66. In a third analysis using binary logistic regression, the sign of error showed some correlation with aspect and minimum extremity, with 55-65% of the original error sign modelled correctly, depending on the test area. All parameters that exhibited a significant correlation with either error or error magnitude were included in a stepwise regression analysis. The best fit for modelling error was achieved with three parameters (mean extremity, curvature and aspect) yielding an r^2 of around

0.23. Regression of the magnitude of error gave an average r^2 of 0.42 (Table 4) using only two variables roughness (altitude) and minimum extremity. Taking the mean of the corresponding factors from all three test areas gave the following regression equation for modelling the amount of error:

$$abs(\varepsilon) = 0.53 \times roughness + 0.031 \times extremity_{min} + 7.6 \quad (1)$$

This regression was found to capture 50-70% of the measured error magnitude for the three test areas. As results of regression on error were considerably weaker, only the regression on error magnitude was used in the uncertainty model. Slope and its derivatives are therefore not used in the model and the analysis was continued on the unprojected WGS84 datasets.

Using 1, residuals were calculated for the three test areas and analysed. Residuals showed to be centered around a mean of 0 with a standard deviation of 43-50m, minimum values of around -300m and their maxima at 600-900m. This resulted in mildly skewed (skewness 1.7-2.4) distributions with high kurtosis of 10-18. The residuals were found to be well approximated using a modified random normal distribution ($N[0, 45]$). Squaring the residuals and randomly reassigning the signs to center the distribution around 0 again, then downscaling through a division by 100 proved to be a simple and satisfactory way to simulate regression residuals, while introducing a stochastic component to the uncertainty model.

Since only the magnitude of error showed a useful correlation, the sign of the modelled uncertainty was modelled separately for the uncertainty model. Although equation (2), derived from binary logistic regression showed agreement of only 55-65% of modelled against true error sign, the regression proved to capture the spatial correlation of the error sign well, at the cost of an overestimation of positive error of the order of 10-20%:

$$S = -0.0012 \times extremity_{mean} + 0.002 \times aspect - 0.2 \quad (2)$$

where $-1 \leq S \leq 1$. Further analysis confirmed that the closer the modelled values were to either +1 or -1, the higher the probability that the error's sign was modelled correctly. For the three test areas, almost all values higher than 0.6 or lower than -0.6, respectively, modelled the error sign correctly. Thus, a stochastic element was introduced for modelling error sign, where a random number r was drawn from a standard normal distribution for every value of S . Where $r \leq abs(S) + f$, with the correction factor $f = 0.35$, the modelled sign was kept, otherwise the sign was assigned randomly. This resulted in a ratio of positive to negative modelled error close to the measured error, while retaining most of the spatial characteristics of the sign distribution.

Combining the three steps, that is modelling the dependence of the error, residuals (*resid*) and error sign resulted in the following uncertainty model:

$$U_{tot} = (abs(\varepsilon) + resid) \times S \quad (3)$$

Finally, the modelled surfaces, though correctly representing the statistical distribution of error, did not yet take full account of the spatial autocorrelation of error. A Gaussian convolution filter (Oksanen and Sarjakoski, 2005) was thus applied to the modelled uncertainty raster by transforming the distribution of modelled uncertainty to a normal distribution and applying a convolution filter with a kernel range of 3km (3cells). After the filtering, the uncertainty raster was transferred back to its original distribution. QQ-plots show the distribution to be altered only minimally, with the added advantage that unrealistically noisy parts of the surface were effectively smoothed.

Modelled uncertainty surfaces Modelled uncertainty surfaces show a good correspondence in spatial configuration with the de-

	Mean	Max	Min	STD	Skew.	Kurt.	Sum
Mean	0.64	560	-561	40.5	0.0	8.7	$3.8E^6$
STD	0.02	54.8	53.7	0.02	0.0	0.03	$8.9E^4$

Table 5: Mean and standard deviation of the distribution statistics of 100 modelled uncertainty surfaces for Fennoscandia. Uncertainty modelled in meters.

derived error surfaces (Figure 3). The general dependencies visible in the derived error surfaces (Figure 3A) are generally preserved in the modelled uncertainty (Figure 3B), due to the regression component of the model. The small scale distribution of modelled uncertainty is generally noisier than that of the error, with the autocorrelation introduced through convolution filtering clearly visible (Figure 3B, inset). Comparing the histograms of

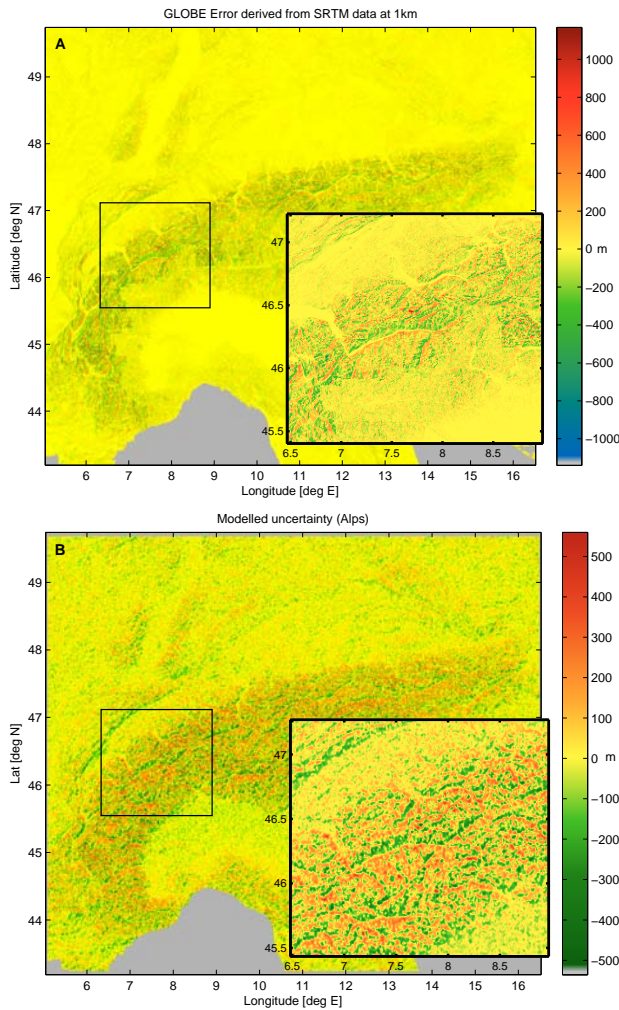


Figure 3: GLOBE error surfaces for the Alps derived using SRTM reference data (A), and modelled uncertainty surface (B) both with detail inset.

the derived error with the modelled uncertainty (Figure 4) shows good accordance, with an underestimation of values close to zero and an overestimation of values around the standard deviation of the distribution. Extreme error values are not reproduced by the uncertainty model, and the overall sum of the modelled uncertainty for any of the test areas is within 10% of the range of derived error. Modelling a suite of 100 uncertainty surfaces for Fennoscandia (2366x2576 cells), the descriptive statistics proved to vary little (Table 5). Calculating the mean, range and standard deviation of the modelled uncertainty for every raster cell across all 100 runs (Figure 5) illustrates the influence of the de-

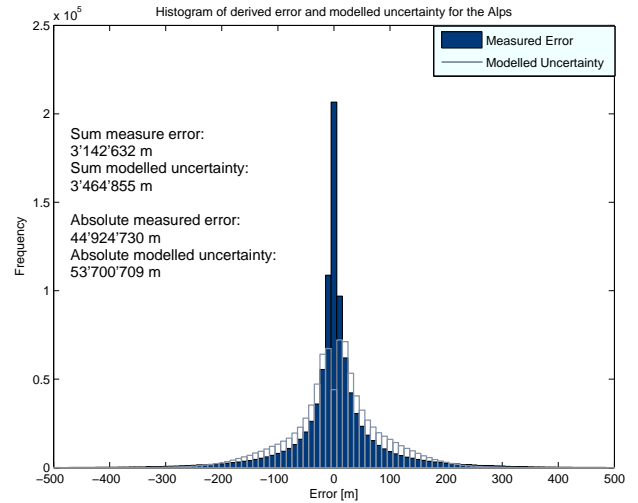


Figure 4: Histogram of the derived error for the Alps test area, compared to that of an example of a stochastically generated uncertainty surface for the same area.

terministic and the stochastic parts of the uncertainty model. For areas with mean positive or negative error, the strong influence of the sign regression results in predominately positive or negative errors. Likewise, areas of high uncertainty are likely to be the result of the regression modelling the magnitude of error following dominant landscape features. However, the two stochastic elements in the determination of error sign and modelling of the residuals introduce a stochastic component that results in imposition of noise across the raster, shown through the standard deviation and range of modelled uncertainty (Figure 5c,d).

3.2 Sensitivity study

Figure 6 and Figure 7 show a suite of representations of the influence of the modelled uncertainty in ISM results as a result of the driving temperature (Figure 6b) imposed together with the parameterisation of mass balance. Figure 6 shows the development through time of ice sheet extent and volume and the uncertainty induced in these values as a function of the DEM uncertainty, while Figure 7 illustrates the variation in ice sheet extent for a variety of snapshots in time.

These results clearly show that, firstly, uncertainty is greatest during ice sheet inception (standard deviation (STD) in extent $\sim 12\%$), where uncertainties in elevation can raise or lower individual ice nucleation centres above or below the ELA. As ice centres grow and coalesce, the effects of uncertainty in topography decrease (STD in extent $\sim 3\%$), as the ice mass itself becomes the predominant topography. However, during periods of retreat (e.g around 20ka model years), uncertainty again increases.

Figure 7 clearly shows how with a mature ice sheet (e.g. after around 37ka model years), most uncertainty in ice sheet extent is found at the edges of the ice sheet. Once the ice sheet has reached a certain size, e.g. after approx 10ka model years, the range of uncertainty in the position of the ice front for these simulations varies between 40-100km for all later model stages. The variation is less at the NW ice front, as the bathymetry rapidly lowers off the Norwegian coast and the ISM ablates ice all ice at altitudes lower than -500m. Variation of ice extent across the MCS runs is thus much higher towards Finland and the Baltic Sea.

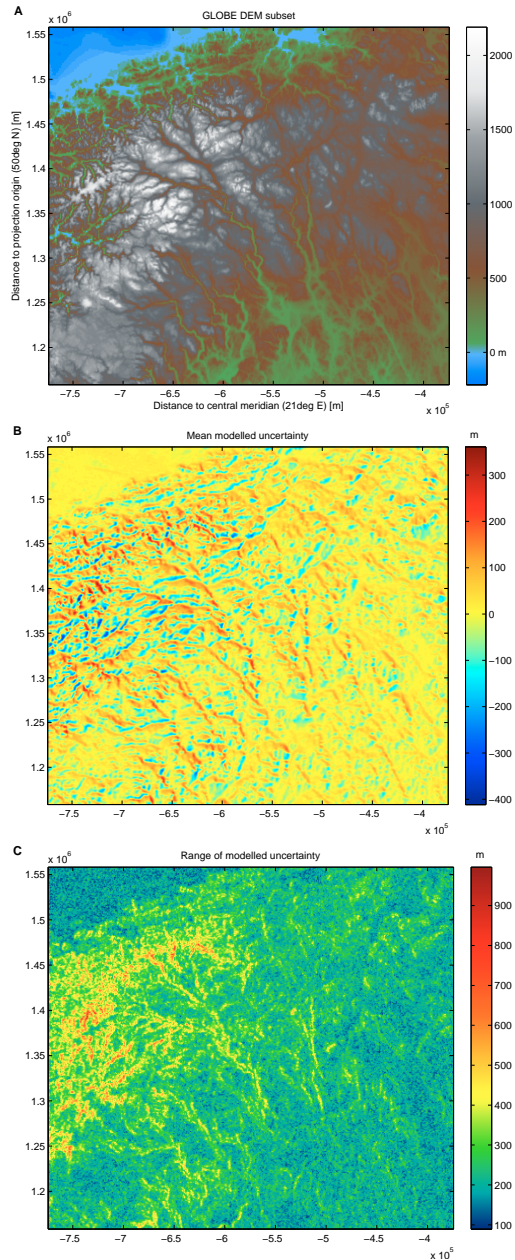


Figure 5: Part of the Fennoscandian DEM (A, inset in Figure 2D), with mean (B) and range (C) of modelled uncertainty for the area averaged over 100 surfaces.

4 DISCUSSION

In Section 1.2 we set out three broad aims for this work, namely to quantify DEM error for a variety of regions where higher quality data were available, to develop a general model of uncertainty based on these findings and, to apply this model to assess the uncertainty introduced into the results of ISM runs as a result of uncertainty in DEMs.

4.1 Quantifying DEM error

In assessing DEM error, we sought to identify areas which had broadly similar characteristics, based on the assumption that dependencies and characteristics of DEM error based on a DEM might be expected to be broadly similar for similar regions. Table 5 gives the descriptive statistics for error surfaces calculated

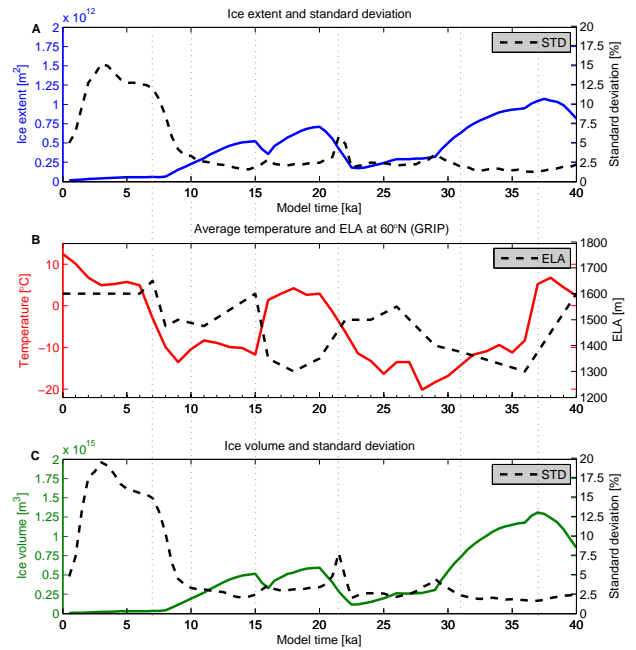


Figure 6: Mean ice extent (A) and volume (C) with their respective relative standard deviation (dashed lines) across 100 MCS runs plotted against modelling time. Climate forcing (temperature and ELA) shown in B, with vertical gray lines marking snapshot times shown in Figure 7.

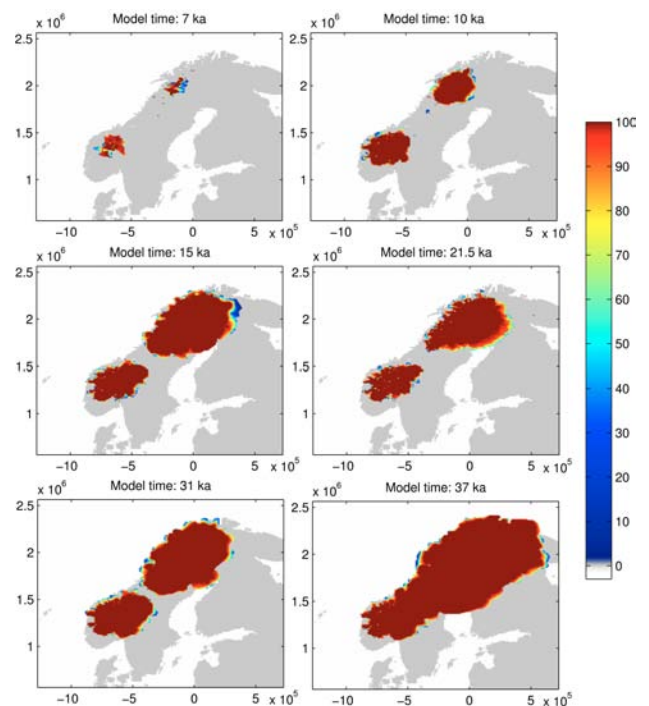


Figure 7: Frequency of DEM cells glaciated across 100 MCS runs after 7, 10, 15, 21.5, 31 and 37ka modeltime. Present time Fennoscandian coastline plotted for comparison.

for the three regions, which are broadly similar suggesting that this assumption is reasonable.

However, a further inherent assumption is that the variation in error is mainly described by terrain parameters within each region. In fact, this was found not to be the case in the Alpine region,

where error values notably decreased at the Swiss/Italian border in the Italian region of the Alps, where the original GLOBE data has a different source.

The error surfaces themselves (e.g. Figure 3a) show strong correlations of error with terrain features and, most strikingly, that error increases and is more spatially autocorrelated in areas of high relief. Initial attempts to correlate error with a range of parameters were relatively unsuccessful with low correlations, however the absolute error was found to be relatively strongly correlated with roughness and minimum extremity. Roughness in particular increases with relief, thus suggesting that the use of such a parameter is sensible. Local models with different coefficients were averaged for the 3 regions to create a global model (Equation 1) and the differences between the r^2 values generated by the local and global models found to be small, thus justifying the application of this global model in areas with similar terrain characteristics.

Examination of the residuals for the error model showed that no correlations with terrain parameters and no spatial autocorrelation. Thus this component of the error model was treated as uncertainty, along with the sign of the magnitude of error and is discussed further below.

The sign of the magnitude of the error was also examined for correlation with terrain parameters, and weak dependencies found (around 55-65% of the signs were correctly modelled by a binary logistic regression) based on aspect and mean extremity. These parameters, in particular aspect, introduce spatial autocorrelations to the error model similar to those seen running along terrain features. However, as discussed in Section 3.1 a purely deterministic approach to modelling error sign significantly overestimates positive errors, and thus a further stochastic term was introduced.

4.2 Developing an uncertainty model

The uncertainty model given in Equation 3 has three terms - absolute error, a residual and error sign. Of these 3 terms the first is purely deterministic, whilst the latter both contain stochastic elements, resulting in the generation of an uncertainty model.

Importantly for our application, the uncertainty model can be generated purely from a single DEM, thus allowing us to model uncertainty in regions where high quality data are not available. Figures 3 and 4 show a comparison between one uncertainty surface for the Alps and calculated error for the same region. The influence of the stochastic elements is immediately clear, with considerably more noise in areas of lower relief and overall, and overall greater total error (i.e the area under the curve in Figure 4). However, the range of error for the uncertainty surface is lower than that for the calculated error and the sum of positive and negative values (see Figure 4) similar.

Figure 5 shows how the uncertainty surfaces for Fennoscandia are themselves related to terrain features. For example, the mean modelled uncertainty is greatest in regions of high relief. The range of uncertainty illustrates clearly that areas where ice sheet inception is likely have the highest uncertainty in elevation (of the order of 800m).

The application of the convolution filter effectively smoothes extreme outliers and reduces the range of uncertainty within a given distance. This is important in many modelling applications, since outliers in particular, can lead to model instabilities (e.g. through unphysically steep slopes for a given resolution).

One important limitation of the model as it stands, lies in the similarity between the three test regions and Fennoscandia. Overall, Fennoscandia has less and lower areas of high relief by comparison to our three test regions, and therefore uncertainty may be overestimated. However, as long as this assumption is clearly stated, we believe that the application of the model is

valid.

Since for Fennoscandia no higher accuracy reference data is available, other approaches of modelling DEM uncertainty including autocorrelation, such as stochastic conditional simulation (Kyriakidis et al., 1999) would be difficult to implement. However, if a measure of spatial autocorrelation of the error could be correlated to DEM attributes or compound indices, local information on spatial correlation could be used for improving the uncertainty surfaces produced, e.g. by using automated variogram analysis with stochastic conditional simulation (Liu and Jezek, 1999).

4.3 Case study - ISM in Fennoscandia

The developed uncertainty model proved to deliver surfaces that are both suitable for Monte Carlo Simulations through the inherent stochastic elements, as well as fit to run an ISM at a considerably low resolution of 10km. Earlier experiments (Hebeler and Purves, 2004) have shown that uncertainty modelled using random error in excess of 100m STD can destabilise the ISM at resolutions as low as 20km. This effect is mainly due to unreasonably high slope gradients introduced by the added uncertainty. By contrast the uncertainty model presented in this paper produces topographically sound surfaces by both incorporating information on the underlying topography as well as convolution filtering, thus avoiding unrealistic terrain configurations.

With a mean of zero and standard deviation of 40m, the introduced uncertainties for Fennoscandia are effectively smaller than those with standard deviations of up to 150m of previous experiments (Hebeler and Purves, 2005), but nevertheless prove to result in significantly different model results, especially during inception and retreat phases of the ISM. This implies that care has to be taken when interpreting results during these phases (Sugden et al., 2002). DEM uncertainties can influence model results in both ice sheet size and configuration during susceptible stages that may otherwise be attributed to climate or mass balance changes.

On the other hand, even though the relative variation of large ice sheets, e.g. the reconstructed Fennoscandian ice sheet after 15k and 31k model years, are relatively small in the order of 2-5% (Figure 6), the absolute difference in modelled extent is the order of 50-100km. Differences of modelled and empirically derived ice extent of ice sheets during the LGM of this order of magnitude have fueled debate over years (Hulton et al., 2002, Wenzens, 2003). In order to relate the impact of these DEM uncertainties to the effect other parameters have on ISM results, further sensitivity studies are necessary. For example stepwise variation of climate forcing, e.g. temperature and mass balance, could be applied and compared to the range of modelled ice sheet configurations this paper delivered.

5 CONCLUSIONS

In this paper, we have successfully captured the dependency of GLOBE DEM error for mountainous terrain with the underlying topography and to integrate this relationship into an uncertainty model. By applying this uncertainty model we produced spatially correlated, realistic uncertainty surfaces that are suitable for the use in Monte Carlo Simulations. Even though the amount of DEM uncertainty derived from GLOBE data was shown to have significant impact on ISM results for the Fennoscandian ice sheet during the LGM, sensitivity studies of ISM parameters and climate forcing are needed to relate the impact of DEM uncertainty e.g. to that of temperature change.

Future experiments will explore whether the developed uncertainty model could be improved by refining the selection of test

areas or through a better reproduction of local spatial autocorrelation. Porting the uncertainty model to other topographies and source data, and testing it on different resolutions, for example using SRTM and LIDAR data, will allow us to explore the sensitivity of other process models to DEM uncertainty.

ACKNOWLEDGEMENT

Felix Hebeler would like to thank Dr Phaedon Kyriakidis, UC Santa Barbara, Prof Peter Fisher and Dr Jo Wood (both City University London) as well as Dr Juha Oksanen (Finnish Geodetic Institute) for their advice and encouragement. This research is funded by the Swiss National Science Foundation (SNF Project Number 200021-100054).

REFERENCES

- Carlisle, B. H., 2000. The highs and lows of DEM error - developing a spatially distributed DEM error model. In: Proceedings of the 5th International Conference on GeoComputation, University of Greenwich, United Kingdom, pp. 23–25.
- CIAT, 2006. International Centre for Tropical Agriculture: Void-filled seamless SRTM data V3, available from the CGIAR-CSI SRTM 90m Database: <http://srtm.csi.cgiar.org>.
- Ehlschlaeger, C. R., Shortridge, A. M. and Goodchild, M. F., 1997. Visualizing spatial data uncertainty using animation. *Computers & Geoscience* 23(4), pp. 387–395.
- Fisher, P. F. and Tate, Nicholas, J., 2006. Causes and consequences of error in digital elevation models. *Progress in Physical Geography* 30(4), pp. 467–489.
- GLOBE Task Team & others, 1999. The Global Land One-kilometer Base Elevation (GLOBE) Digital Elevation Model, Version 1.0. Digital data base on the World Wide Web (URL: <http://www.ngdc.noaa.gov/mgg/topo/globe.html>) and CD-ROMs. National Oceanic and Atmospheric Administration, National Geophysical Data Center, 325 Broadway, Boulder, Colorado 80303, U.S.A.
- Hagdorn, M. K. M., 2003. Reconstruction of the Past and Forecast of the Future European and British Ice Sheets and Associated Sea-Level Change. unpublished PhD thesis, University of Edinburgh.
- Hagdorn, M., Rutt, I., Payne, T. and Hebeler, F., 2006. GLIMMER - The GENIE Land Ice Model with Multiply Enabled Regions - Documentation. <http://glimmer.forge.nesc.ac.uk/>. Universities of Bristol, Edinburgh and Zurich.
- Harding, D. J., Gesch, D. B., Carabajal, C. C. and Luthcke, S. B., 1999. Application of the shuttle laser altimeter in an accuracy assessment of GTOPO30, a global 1-kilometer digital elevation model. *International Archives of Photogrammetry and Remote Sensing*. 17-3/W14, pp. 81–85.
- Hastings, D. A. and Dunbar, P. K., 1998. Development & assessment of the global land one-km base elevation digital elevation model (GLOBE). *ISPRS Archives* 32(4), pp. 218–221.
- Hebeler, F. and Purves, R. S., 2004. Representation of topography and its role in uncertainty: a case study in ice sheet modelling. In: *GIScience 2004: Proceedings of the third international conference on geographic information science*, pp. 118–121.
- Hebeler, F. and Purves, R. S., 2005. A comparison of the influence of topographic and mass balance uncertainties on modeled ice sheet extents and volumes. In: *Eos Trans. AGU, Fall Meet. Suppl.*, Vol. 86, pp. Abstract C23A–1154. No 52.
- Heipke, C., Koch, A. and Lohmann, P., 2002. Analysis of SRTM DTM - methodology and practical results. In: A. Boberg (ed.), *Journal of the Swedish Society for Photogrammetry and Remote Sensing: Photogrammetry meets geoinformatics*, Vol. 2002:1, pp. 69–80.
- Holmes, K. W., Chadwick, O. and Kyriakidis, P., 2000. Error in a USGS 30-meter digital elevation model and its impact on terrain modeling. *Journal of Hydrology* 233, pp. 154–173.
- Hulton, N. R., Purves, R. S., McCulloch, R., Sugden, D. E. and Bentley, M., 2002. The Last Glacial Maximum and deglaciation in southern South America. *Quaternary Science Reviews* 21, pp. 233–241.
- Hunter, G. J. and Goodchild, M. F., 1997. Modelling the uncertainty of slope and aspect estimates derived from spatial databases. *Geographical Analysis* 19(1), pp. 35–49.
- IPCC, 2001. *Climate Change 2001: Synthesis Report. A Contribution of Working Groups I, II, and III to the Third Assessment Report of the Intergovernmental Panel on Climate Change*. Cambridge University Press, Cambridge, United Kingdom, and New York, NY, USA.
- Jarvis, A., Rubiano, J., Nelson, A., Farrow, A. and Mulligan, M., 2004. Practical use of SRTM data in the tropics: Comparisons with digital elevation models generated from cartographic data. Working Document 198, Cali, International Centre for Tropical Agriculture (CIAT): 32.
- Kyriakidis, P. C., Shortridge, A. and Goodchild, M., 1999. Geostatistics for conflation and accuracy assessment of digital elevation models. *International Journal of Geographical Information Science* 13(7), pp. 677–707.
- Liu, H. and Jezek, K. C., 1999. Investigating dem error patterns by directional variograms and fourier analysis. *Geographical Analysis* 31, pp. 249–266.
- Marshall, S. J., 2002. Modelled nucleation centres of the pleistocene ice sheets from an ice sheet model with subgrid topographic and glaciologic parameterizations. *Quaternary International* 95-96, pp. 125–137.
- Montgomery, D. R., 2001. Slope distributions, threshold hillslopes, and steady-state topography. *American Journal of Science* 301(4-5), pp. 432.
- Oksanen, J. and Sarjakoski, T., 2005. Error propagation of DEM-based surface derivatives. *Computers & Geoscience* 31(8), pp. 1015–1027.
- Purves, R. S. and Hulton, N. R., 2000. Experiments in linking regional climate, ice-sheet models and topography. *Journal of Quaternary Science* 15, pp. 369–375.
- Sugden, D. E., Hulton, N. R. and Purves, R. S., 2002. Modelling the inception of the patagonian icesheet. *Quaternary International* 95-96, pp. 55–64.
- Sun, G., Ranson, K. J., Kharuk, V. I. and Kovacs, K., 2003. Validation of surface height from shuttle radar topography mission using shuttle laser altimeter. *Remote Sensing of Environment* 88(4), pp. 401–411.
- Wechsler, S. P., 2006. Uncertainties associated with digital elevation models for hydrologic applications: a review. *Hydrology and Earth System Sciences Discussions* 3, pp. 2343–2384.
- Weng, Q., 2002. Quantifying uncertainty of digital elevation models derived from topographic maps. In: D. Richardson and P. van Oosterom (eds), *Advances in Spatial Data Handling*, Springer, chapter 30, pp. 403–418.
- Wenzens, G., 2003. Comment on: 'The Last Glacial Maximum and deglaciation in southern South America' by N.R.J. Hulton, R.S. Purves, R.D. McCulloch, D.E. Sugden, M.J. Bentley [*Quaternary Science Reviews* 21 (2002) 233–241]. *Quaternary Science Reviews* 22(5-7), pp. 751–754.
- Wood, J. D., 1996. The Geomorphological Characterisation of Digital Elevation Models. PhD thesis, University of Leicester, UK.